symmetry

Article

Note about Passive Continuous Variable Quantum Key Distribution over Turbulent Atmospheric Channel

Yun Mao [1,2,†], Yiwu Zhu [2,†], Yijun Wang [2,*] and Ying Guo [2,3,*]

1 School of Information Engineering, Shaoyang University, Shaoyang 422000, China
2 School of Automation, Central South University, Changsha 410083, China
3 School of Computer Science, Beijing University of Posts and Telecommunications, Beijing 100876, China
* Correspondence: xxywyj@csu.edu.cn (Y.W.); guoying@bupt.edu.cn (Y.G.)
† These authors contributed equally to this work.

Abstract: Continuous variable quantum key distribution (CVQKD) has been implemented over the atmospheric channels over free space. However, atmospheric turbulence weakens the quality of the transmitting quantum signals and hence decreases the secret key rate of the system. Here, we suggest an atmospheric turbulence channel model that involves atmospheric turbulence bubbles and demonstrates the implementation feasibility of passive CVQKD with spectrum resources in the terahertz band over the atmospheric turbulence channel. We achieve the channel transmittance characterized by the refractive index and the wavefront distortions. Moreover, an adaptive optics (AO) unit is used for performance improvement while considering the effect of the thermal noise and excess noise on the atmospheric turbulence bubble-modeled channel. Numerical simulations show that the AO-involved detection scheme can result in reductions in excess noise when being faced with the floating clouds and mist in atmospheric turbulence, which results in performance improvements in terms of secret key rate, which confirms the utility of the high-rate and long-distance CVQKD in terahertz (THz) for practical implementations.

Keywords: quantum key distribution; adaptive optics; atmospheric turbulence; quantum communications

Citation: Mao, Y.; Zhu, Y.; Wang Y.; Guo, Y. Note about Passive Continuous Variable Quantum Key Distribution over Turbulent Atmospheric Channel. *Symmetry* **2022**, *14*, 2128. https://doi.org/10.3390/sym14102128

Academic Editor: Christos Volos

Received: 19 September
Accepted: 10 October 2022
Published: 13 October 2022

1. Introduction

Quantum key distribution (QKD) is a branch of quantum communications [1–4] where two trusted communicators including Alice and Bob are bound to share a string of secret keys at random through a public quantum channel. QKD includes discrete-variable (DV) QKD [1,2] and continuous-variable (CV) QKD [3,4]. The former encodes information of key bits in the polarization states of a single photon, whereas the latter encodes information symmetrically with two quadratures ($\hat{x}$ and $\hat{p}$) of the optical field both with Gaussian modulation, whose theoretical security in the finite-size regime and asymptotic limit has been proven successively over a long distance.

Recently, large quantities of CVQKD protocols have been proposed in free-space links, such as satellite-to-satellite links, satellite-to-ground links [5,6], and so on. Unfortunately, the transmission coefficient fluctuates due to effects of the atmospheric turbulence, and hence the coherent detection may be distorted, which involves not only the wavefront and amplitude of laser carrier signal but also transmission attenuation, shortening the transmission distance of CVQKD [7,8]. To model the atmospheric turbulence channel, several scenarios of turbulence have already been proposed [9,10], including beam wandering, randomly blocked and log-normal distribution, which demonstrates the evolution of the receiving beam in weak and strong turbulence. However, there is no suitable atmospheric channel model that can illustrate effect of floating clouds and mist in turbulence. In what follows, we will establish an atmospheric bubble-modeled channel that can describe the suitable effect of the floating cloud and mist in turbulence with geometric optics to conceive the propagation process of optical or microwave photons.

There are two contributions towards this work. On the one hand, we suggest an approach to description of effect of the floating cloud and mist in atmospheric turbulence while establishing a suitable atmospheric turbulence bubble-modeled channel, whereas, on the other, we counteract the effect of the channel-added noise by employing an AO unit, which can efficiently compensates for the channel-added noise generated from the imperfect detector at the receiver, leading to the performance improvement of the practical CVQKD in the terahertz band.

This paper is organized as follows. In Section 2, we introduce literature reviews in order to illustrate the background of CVQKD with passive state preparation. In Section 3, we propose the scheme of AO-based FS-CVQKD in the THz band over the atmospheric turbulence channel. Given the clouds and mist in the atmospheric turbulence, we suggest an atmospheric turbulence bubble-modeled channel, which is combined with the traditional elliptic-beam model in Section 4. In Section 5, we consider the character of a turbulence bubble-modeled channel for FS-CVQKD using numerical simulations and demonstrate its effect on the security of the AO-based FS-CVQKD. Finally, conclusions are drawn in Section 6.

2. Literature Reviews

For the classical CVQKD protocol [11], quantum states are prepared actively, and thus it is usually called active CVQKD. The CVQKD system with active state preparation [12], as shown in Figure 1, can be designed as follows:

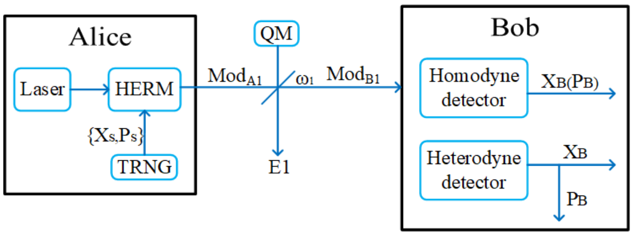

Figure 1. CVQKD protocol with active state preparation. QM is a quantum memory device which is used to store the outputs from Eve; HERM denotes the high extinction ratio modulator; TRNG denotes true random number generator; ω_1 is the variance of thermal noise; and E_1 is ancillary modes.

Step 1: There is a laser generator on Alice's side, which produces light as an information carrier. For every transmission, the TRNG will randomly generate a pair of numbers that satisfy the Gaussian distribution. The light that Alice produces then goes through a high-extinction-ratio Gaussian modulator. By adjusting the phase and amplitude of the light, Alice prepares a coherent state with Gaussian modulation.

Step 2: Alice sends her coherent states to Bob through an atmospheric turbulence channel, which can be attacked by Eve.

Step 3: After Bob receives the coherent state from Alice, he chooses to either measure one of the two quadratures at random or measure both of the quadratures.

Step 4: After they complete communications of quantum transmission, Alice and Bob process the raw keys in a series of ways, such as reconciliation, error correction, and privacy amplification. Finally, they achieve the final keys.

According to the aforementioned active CVQKD [13], it requires a highly precise modulator to meet the constraints of complex modulation format while suppressing the modulation errors, making it difficult to lay a portable terminal device for quantum network. In order to solve this problems in practical implementations, the QKD with passive state preparation was proposed in 2007 [14], which is called a passive DVQKD that can be implemented with the single photon source.

Different from the active CVQKD for state preparation, the working principles of the passive CVQKD, as shown in Figure 2, can be described as follows:

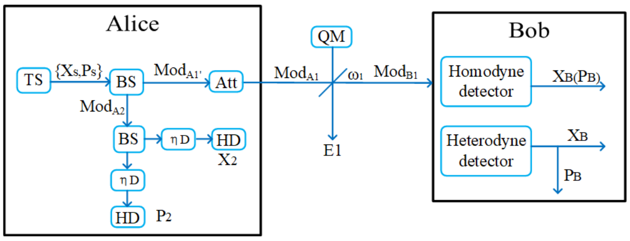

Figure 2. CVQKD protocol with passive state preparation. TS is the thermal source; BS denotes the beam splitter; HD means homodyne detector; Att is optical attenuator; and η_D is the transmittance of the beam splitter.

Step 1: Alice splits the output of the thermal source into two spatial modes, $\mathrm{Mod}_{A1'}$ and Mod_{A2}, through the beam splitter (BS). She chooses one of the two spatial modes $\mathrm{Mod}_{A1'}$ and measures both of the two quadratures.

Step 2: Alice transmits another spatial mode Mod_{A2} to Bob after performing the appropriate optical attenuation.

Step 3: Alice can learn the quadrature value of Mod_{A2} through scaling down the measurement results by using an optical attenuator.

Step 4: The actions on Bob's side are the same as before. There is a correlation between the measurements of Alice and Bob. Finally, they can figure out a secret key after further works.

Compared with active state preparation, which requires high-extinction-ratio modulators to reduce the modulation's deviation, the passive state comes from a thermal state, which means the sender just needs a thermal source rather than performing Gaussian modulation to a coherent state to generate a specific thermal source [15,16].

We note that for the Gaussian-modulated coherent states (GMCS) in the active CVQKD, the randomness comes from true random number generator, whereas in the passive CVQKD, the randomness comes from the correlated thermal states which are split from a common thermal source [17]. The former allows the entanglement source to be controlled by Eve while the latter requires a trusted source. Moreover, in the active CVQKD, Alice requires a high-extinction-ratio modulator to adjust the phase and amplitude of the light, which makes it different to realize in practice. However, in the passive CVQKD, it just need two homodyne detectors, resulting in the easy implementation of CVQKD in practice [18].

Currently, the passive state preparation has drawn a lot of attention [19,20], but it has been only focused on DVQKD. However, the passive quantum state preparation in CVQKD was suggested in 2018 [21] and has been subsequently proven in both theoretical studies and in experiments [22–24].

So far, CVQKD has been carried out over free space (FS) in the terahertz (THz) band, and it turns out to be potentially able to meet the needs of high-rate quantum communications [25]. However, due to effects of environmental thermal noise, the security threshold of the THz CVQKD is still high in terms of the secret key rate as well as the maximal transmission distance [26,27]. Fortunately, the atmospheric turbulence can be efficiently compensated by deploying a suitable adaptive optics (AO) unit to mitigate the turbulence wavefront aberrations of the received laser carrier signals. In what follows, we will consider effect of the AO unit on the passive CVQKD over an atmospheric turbulence channel while taking into account the atmospheric turbulence bubble-modeled channel, which provides an interesting theoretical model for the THz quantum communications.

3. Passive CVQKD Embedded with an AO Unit

As for its implementation over an atmospheric channel, it can be described as follows. As shown in Figure 3, we suggest a schematic diagram of the passive CVQKD embedded with an AO unit, which involves the thermal state in THz band, transmitting over an atmospheric turbulence channel.

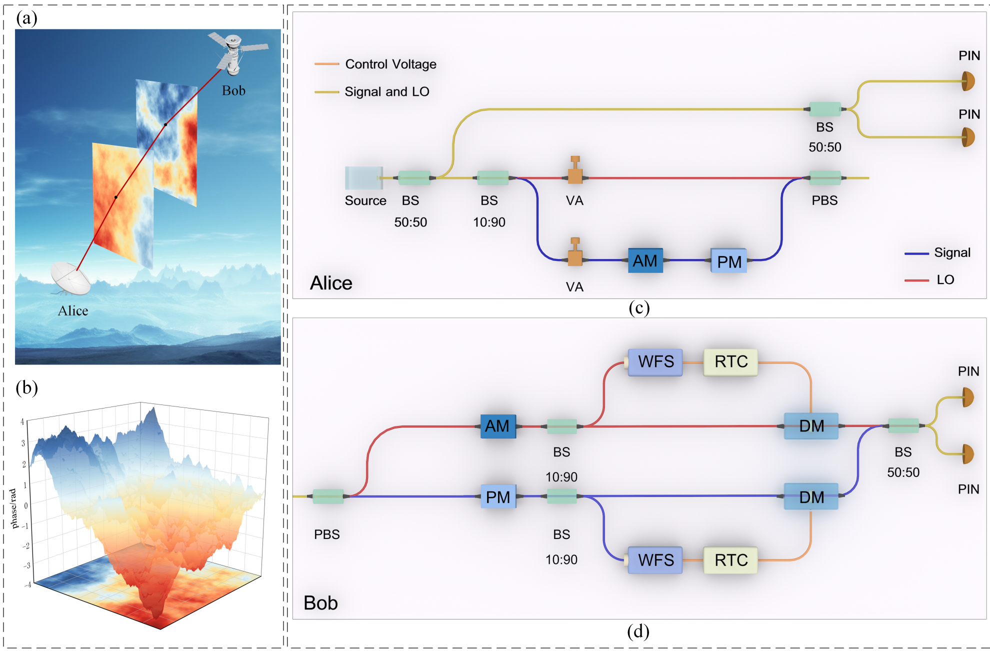

Figure 3. (**a**) The AO-based CVQKD system in the atmospheric channel. (**b**) The phase diagram in the atmospheric channel. (**c**) Schematic diagram of Alice's preparation setup. (**d**) Bob's detection detection setup. BS: beam splitter. PBS: polarization beam splitter. AM: amplitude modulator. VA: voltage attenuator. PM: phase modulator. WFS: wavefront sensor. RTC: real-time controller. DM: deformable mirror. PIN: PIN photodiode.

Alice prepares for the Gaussian-modulated thermal state using the THz source. She performs the Gaussian modulation with two quadrature components, involving amplitude quadrature (x) and phase quadrature (p). The overall variance that includes the shot noise and modulation variance is given by $V = V_A + V_0$, where V_A is the zero-centered Gaussian-distributed modulation variance, and V_0 is the shot noise described as $V_0 = 2\overline{n}_0 + 1$. The parameter $\overline{n}_0$ is represented as:

$$\overline{n}_0 = \frac{1}{\exp(fh/k_b) - 1}, \tag{1}$$

where f denotes the carrier frequency, h is the temperature and k_b is Boltzmann's constant. The shot noise fluctuates due to thermal fluctuations and modulation. Alice measures the coherent states projected on one mode, while she projects another state, transmitting through the untrusted channel. The signal and local oscillator (LO) pulses are split by a 50:50 beam splitter, one part of which is used for homodyne detection and another part of which iz split by a 90:10 beam splitter. The LO path is attenuated before being modulated by amplitude modulator and phase modulator, while the signal path is only attenuated by the attenuator before being multiplexed by PBS.

At the receiver, Bob measures the weak quantum signal with the aid of the strong LO in a shot-noise-limited homodyne or herterodyne detector. Upon receiving the signal and LO pulses, he demultiplexes the pulses with PBS. An AM is applied on the signal path to randomly attenuate the amplitude for shot-noise estimation. Before performing detection, an AO unit is applied on the signal path and LO path to measure and correct wavefront wavefront distortions to restore signal quality and increase the secret key rate by flattening the distorted wavefront. After that, Bob performs optical coherent detection to estimate the excess noise.

The AO unit is combined with the wavefront corrector, the wavefront controller and the wavefront sensor. In Figure 3d, the wavefront aberrations of the received beam are measured by the wavefront sensor as the feedback signal. On the basis of the feedback signal, the wavefront corrector controls the wavefront controller. Finally, the wavefront corrector performs wavefront correction. It can be employed to compensate atmospheric turbulence and improve the quality of the beam.

In Figure 4, we show that the proposed AO unit can be regarded as a filter in practice. The quantum signal follows Gaussian distribution in time domain mixed with excess noise in the turbulence channel. Followed by the employed AO unit, which can be performed with the least mean square (LMS)-based adaptive algorithm, we find that the signal can be efficiently recovered while using the homodyne detection at the receiver.

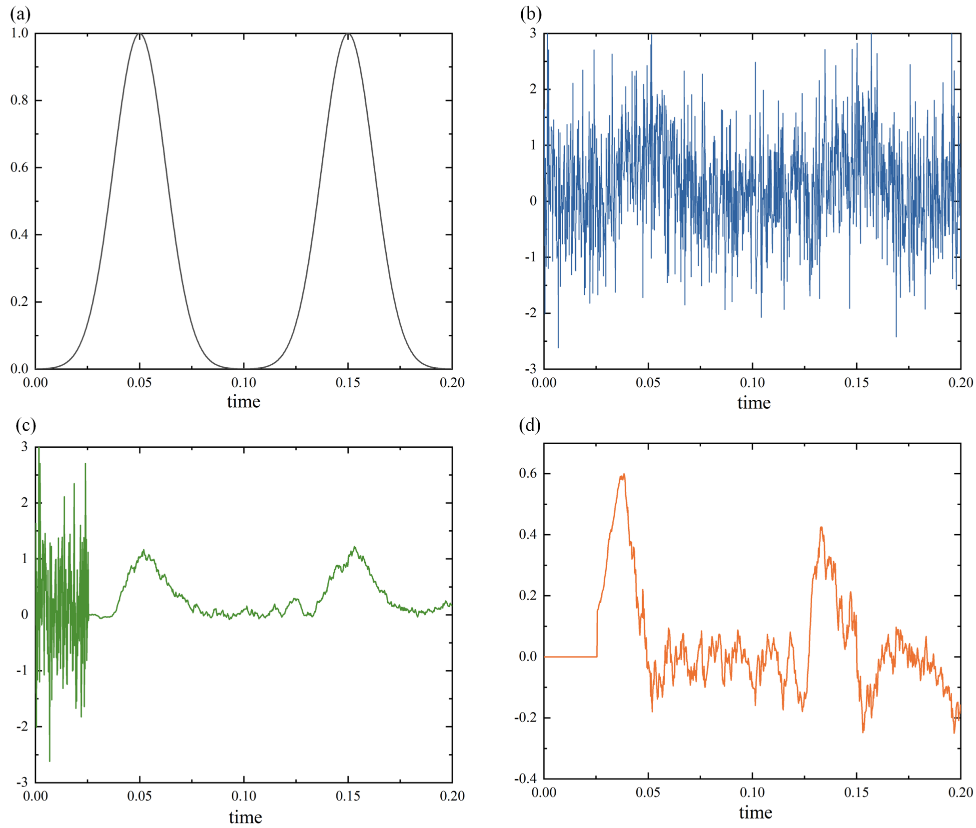

Figure 4. The effect of the proposed AO unit on the transmitted quantum signals in THz band over turbulent atmospheric channel. (**a**) The waveform of the original Gaussian-distributed signal in time domain. (**b**) The waveform of signal mixed with Gaussian-distributed noise in time domain. (**c**) The processed waveform of signal mixed with Gaussian-distributed noise after AO unit in time domain. (**d**) The signal error of the processed signal.

We note that in an AO unit, a wavefront sensor is applied to correct distorted wavefronts by physically distorting the reflective face sheet using mechanical actuators. The closed-loop control system as a feedback to correct atmospheric turbulence, leading to diffraction-limited images. The real-time controller (RTC) instructs the deformable mirror (DM) to adapt to the aberrations. The AO combining electronics with optics can realize the real-time detection of distorted wavefront and then correct distorted wavefronts in real time.

4. Turbulence Bubble-Modeled Atmospheric Channel

The atmospheric turbulence can be modeled with the elliptic-beam model and randomly distributed atmospheric bubbles. The elliptic-beam model has been used for description the atmospheric turbulence in the FS CVQKD [27], while the geometric optics can be applied for conceiving the propagation process of the turbulence bubble-modeled channel.

In the light of the geometric optics, the turbulence model turns out to be a bubble with a refractive index n_2. The varying refraction index contributes to the light refraction as the light crosses the bubble interface. As shown in Figure 5a, the incident ray is refracted on the bubble surface at θ_1, and then the reflected ray travels through the atmospheric channel with the refraction index n_2. Subsequently, the refracted angle reaches θ_2. When the incident ray is not reflected, it follows law of refraction given by:

$$n_1 \sin\theta_1 = n_2 \sin\theta_2. \tag{2}$$

Therefore, we achieve the transmittance ratio T_0 through the turbulence bubble:

$$T_0 = (\cos\theta_1 \cos\theta_2 + \sin\theta_1 \sin\theta_2)^2. \tag{3}$$

As shown in Figure 6, we find that the received noise that is generated from the turbulence bubble-modeled channel for atmospheric channel at the receiver depends on the transmission distance and the modulation variance. For the given modulation variance, the long transmission distance results in the large channel-added noise. The reason for this is that when the atmospheric turbulence gives rise to the fluctuation in the refractive index, the wavefront of the arriving beam is undermined, which degrades the performance of the transmission beam by contributing to beam wandering and the redistribution of energy across the beam section (beam broadening and deformation) [28,29]. The Monte-Carlo method can also be used to illustrate the transmittance as a function of incident angle in Figure 5b. With the decreasing refractive index n_2, the transmittance shows a slighter downward trend.

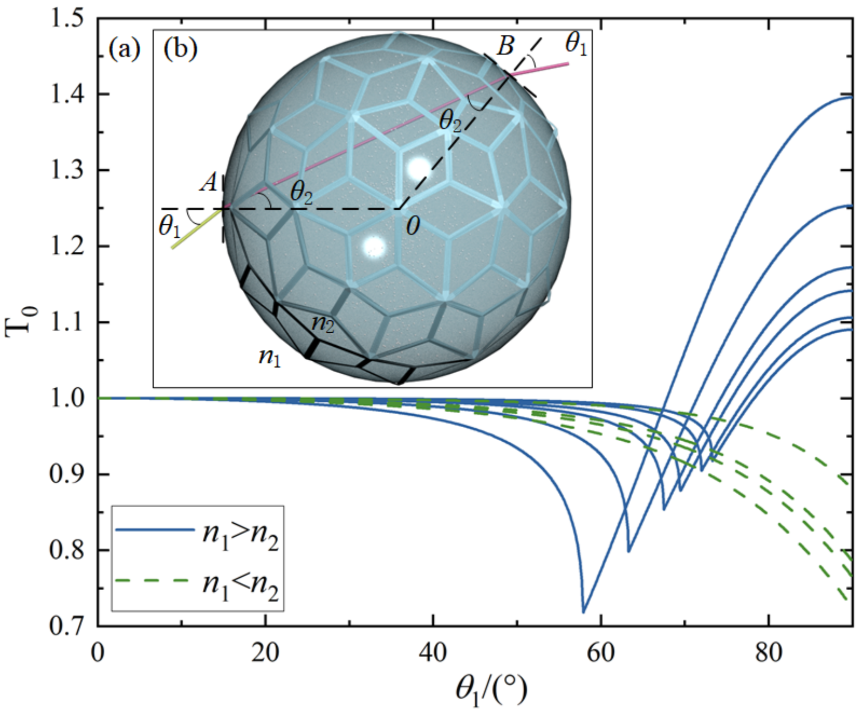

Figure 5. Diagram of the bubble-based atmospheric turbulence channel. (**a**) Continuous refraction of photon over atmospheric turbulence channel. (**b**) The transmittance ratio as a function of incident angle θ_1.

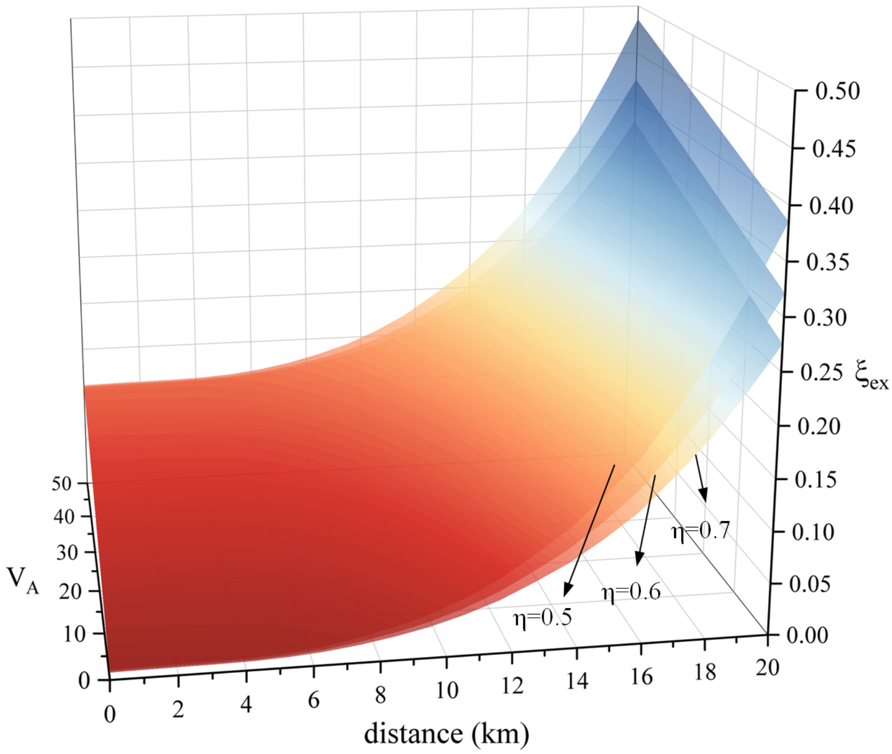

Figure 6. The receiver noise ξ_{ex} as a function of the transmission distance and the modulation variance.

5. Performance Analysis

In what follows, we evaluate the performance of the AO-based CVQKD system while illustrating the influence of the turbulence bubbles model on CVQKD over atmospheric turbulence. In numerical simulations, we take the refracted angle $\theta_1 = 45^\circ$ and the refractive index $n_1 = 1$ in the atmospheric channel. According to the Monte-Carlo simulations in Figure 5b, the transmittance ratio T_0 depends on the refracted index n_2. For $n_2 = 0.8465$, the total reflection achieves the low refractive index, and there are photons transmitted through turbulence bubbles. As the refractive index reaches $n_2 = 1.1753$, the transmittance gradually decreases.

While considering the turbulence bubble-modeled channel for the CVQKD system, we perform numerical simulations, as shown in Figure 7, and the results demonstrate the effects of the refractive index n_2 on the secret key rate of the system. In numerical simulations, we take the closed-loop control frequency as 800 Hz. According to the parameters n_2 in turbulence bubble-modeled channel, the secret key rate of the AO-based CVQKD system has been decreased for $n_2 \in \{1.1753, 0.8465\}$, which is compared with the parameter $n_2 = 1$. For the given transmittance, we find that the deviation in refractive index n_2 has an effect on the secret key rate of the CVQKD system, which confirms the turbulence bubble-modeled channel that can be used to describe the transmission characteristics of atmospheric turbulence.

Furthermore, while deploying a suitable AO unit at the receiver on the signal path and LO path to measure and correct wavefront distortions to enhance the signal quality, the secret key rate of the CVQKD system can be increased by flattening the distorted wavefront, as shown in Figure 8a. We find that the secret key rate of the AO-based CVQKD system has been increased compared with the traditional system. The large transmittance usually results in high secret key rates. In addition, we achieve the total noises involving the channel-added noise, the AO-added noise and the detection-added noise, as illustrated in Figure 8b, where the parameter of the channel-added noise χ_{line} is related to the electrical noise and transmission T and the AO-added noise $\chi_w = 0.65$. We choose the mean detection efficiency of the original protocol as $\gamma_h = 0.7$, which is approximately equal to the actual values. We find that the total noise decreases because of the added AO unit at the receiver. The reason is that the efficiency introduced by AO outweighs the AO-added noise. Since the AO unit realizes the real-time detection and compensation of the distorted wavefront, the quality of the optical signal is improved [30], leading to the performance improvement in the passive CVQKD over the atmospheric turbulence channel. Namely, the AO unit that functions as a filter can be used for quality improvement of the deteriorated signals at the receiver against atmospheric turbulence in quantum communication scenarios.

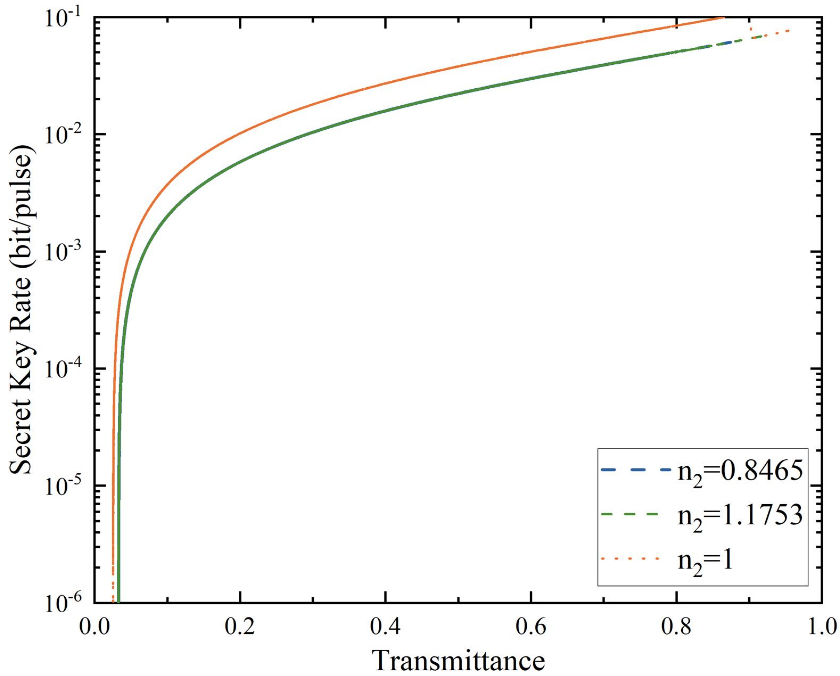

Figure 7. The effect of the refractive index n_2 on performance of the FS CVQKD in the terahertz band over turbulence bubbles.

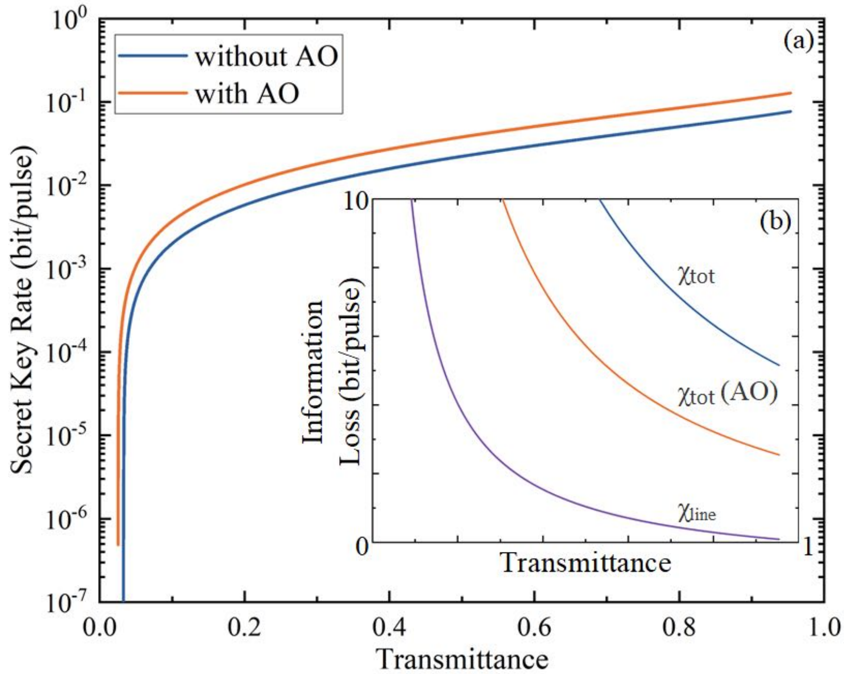

Figure 8. (**a**) The performance of the AO-based CVQKD system. (**b**) The total noise χ_{tot} consists of the channel-added noise χ_{line}, the AO-added noise χ_w and the detection-added noise χ_h. The parameter χ_{line} is related to the electrical noise ϵ_{el} and transmission T.

6. Conclusions

We have developed an atmospheric channel model based on atmospheric turbulence bubble combined with an elliptic-beam model, which provides the feasibility of the passive CVQKD in THz with a high rate and long-distance transmission. We demonstrate characteristics of the atmospheric turbulence bubble-modeled channel involving the refraction index. Taking into account an effect of the channel-added noise and excess noise, we suggest a suitable AO-embedded detector for performance improvement in the passive CVQKD over atmospheric turbulence channel. Numerical simulations show that the performance of the passive CVQKD system can be improved while employing an AO unit in detection to measure and correct wavefront distortions against the atmospheric turbulence. It demonstrates an approach to improve the performance of the THz CVQKD with a high rate and long-distance transmission over atmospheric turbulence. However, the limitation of the turbulence bubble-modeled channel is to create the theoretical sketchy model of quantum communication over atmospheric channel without involving the strict proof in practical implementations. As for its practical security analysis, it is left for our future work based on space modulation devices in experimental implementation of the AO-based CVQKD over atmospheric turbulence.

Author Contributions: Conceptualization, Y.M.; writing—original draft preparation, Y.Z.; writing—review, Y.W.; writing—editing, Y.G. All authors have read and agree to the published version of the manuscript.

Funding: This work was supported by the National Natural Science Foundation of China (Grant Nos. 61871407, 61801522) and the Special Funds for the Construction of an Innovative Province in Hunan (Grant No. 2022GK2016).

Data Availability Statement: All data generated or analyzed during this study are included in this published article.

Conflicts of Interest: The authors declare no conflict of interest.

References

1. Grosshans, F.; Grangier, P. Continuous variable quantum cryptography using coherent states. *Phys. Rev. Lett.* **2002**, *88*, 057902. [CrossRef] [PubMed]
2. Grosshans, F.; Assche, G.V.; Wenger, J.; Brouri, R.; Cerf, N.J.; Grangier, P. Quantum key distribution using gaussian-modulated coherent states. *Nature* **2003**, *421*, 238–241. [CrossRef] [PubMed]
3. Braunstein, S.L.; van Loock, P. Quantum information with continuous variables. *Rev. Mod. Phys.* **2005**, *77*, 513. [CrossRef]
4. Liao, Q.; Xiao, G.; Xu, C.; Xu, Y.; Guo, Y. Discretely modulated continuous-variable quantum key distribution with an untrusted entanglement source. *Phys. Rev. A* **2020**, *102*, 032604. [CrossRef]
5. Vasylyev, D.; Semenov, A.; Vogel, W. Atmospheric quantum channels with weak and strong turbulence. *Phys. Rev. Lett.* **2016**, *117*, 090501. [CrossRef] [PubMed]
6. Guo, Y.; Xie, C.; Liao, Q.; Zhao, W.; Zeng, G.; Huang, D. Entanglement-distillation attack on continuous-variable quantum key distribution in a turbulent atmospheric channel. *Phys. Rev. A* **2017**, *96*, 022320. [CrossRef]
7. Guo, Y.; Xie, C.; Huang, P.; Li, J.; Zhang, L.; Huang, D.; Zeng, G. Channel-parameter estimation for satellite-to-submarine continuous-variable quantum key distribution. *Phys. Rev. A* **2018**, *97*, 052326. [CrossRef]
8. Liu, C.; Zhu, C.; Nie, M.; Yang, H.; Pei, C. Composable security for inter-satellite continuous-variable quantum key distribution in the terahertz band. *Opt. Express* **2022**, *30*, 14798–14816. [CrossRef] [PubMed]
9. Zuo, Z.; Wang, Y.; Mao, Y.; Ye, W.; Hu, L.; Huang, D.; Guo, Y. Quantum catalysis-assisted attenuation for improving free-space continuous-variable quantum key distribution. *J. Phys. B At. Mol. Opt. Phys.* **2020**, *53*, 185501. [CrossRef]
10. Mao, Y.; Huang, W.; Zhong, H.; Wang, Y.; Qin, H.; Huang, D.; Guo, Y. Detecting quantum attacks: a machine learning based defense strategy for practical continuous-variable quantum key distribution. *New J. Phys.* **2020**, *22*, 083073. [CrossRef]
11. Mao, Y.; Wang, Y.; Huang, W.; Qin, H.; Huang, D.; Guo, Y. Hidden-Markov-model-based calibration-attack recognition for continuous-variable quantum key distribution. *Phys. Rev. A* **2020**, *101*, 062320. [CrossRef]
12. Zhang, Y.; Li, Z.; Yu, S.; Gu, W.; Peng, X.; Guo, H. Continuous-variable measurement-device-independent quantum key distribution using squeezed states. *Phys. Rev. A* **2014**, *90*, 052325. [CrossRef]
13. Lo, H.-K.; Curty, M.; Qi, B. Measurement-device-independent quantum key distribution. *Phys. Rev. Lett.* **2012**, *108*, 130503. [CrossRef] [PubMed]
14. Mauerer, W.; Silberhorn, C. uantum key distribution with passive decoy state selection. *Phys. Rev. A* **2007**, *75*, 050305. [CrossRef]

15. Yoritoshi, A.; Takashi, Y.; Masato, K.; Nobuyuki, I. Simple and efficient quantum key distribution with parametric down-conversion. *Phys. Rev. Lett.* **2007**, *99*, 180503.
16. Zhang, Y.; Chen, W.; Wang, S.; Yin, Z.Q.; Xu, F.X.; Wu, X.W.; Dong, C.H.; Li, H.W.; Guo, G.C.; Han, Z.F. Practical non-Poissonian light source for passive decoy state quantum key distribution. *Opt. Lett.* **2010**, *35*, 3393–3395. [CrossRef] [PubMed]
17. Huang, P.; Wang, T.; Chen, R.; Wang, P.; Zhou, Y.M.; Zeng, G.H. Experimental continuous-variable quantum key distribution using a thermal source. *New J. Phys.* **2021**, *23*, 113028. [CrossRef]
18. Qi, B.; Gunther, H.; Philip, G.E.; Brian, P.W.; Ryan, M.C.; Nicholas, A.P. Förster-Resonance Energy Transfer between Diffusing Molecules and a Functionalized Plasmonic Nanopore. *Phys. Rev. Appl.* **2020**, *13*, 054065. [CrossRef]
19. Curty, M.; Ma, X.F.; Lo, H.K.; Lütkenhaus, N. Passive sources for the Bennett-Brassard 1984 quantum-key-distribution protocol with practical signals. *Phys. Rev. A* **2010**, *82*, 052325. [CrossRef]
20. Sun, S.H.; Tang, G.Z.; Li, C.Y.; Liang, L.M. Experimental demonstration of passive-decoy-state quantum key distribution with two independent lasers. *Phys. Rev. A* **2016**, *94*, 032324. [CrossRef]
21. Qi, B.; Evans, P.G.; Grice, W.P. Passive state preparation in the Gaussian-modulated coherent-states quantum key distribution. *Phys. Rev. A* **2018**, *97*, 012317. [CrossRef]
22. Xu, S.J.; Li, Y.; Wang, Y.J.; Mao, Y.; Wu, X.D.; Guo, Y. Security Analysis of a Passive Continuous-Variable Quantum Key Distribution by Considering Finite-Size Effect. *Entropy* **2022**, *23*, 1698. [CrossRef] [PubMed]
23. Wu, X.D.; Wang, Y.J.; Li, S.; Zhang, W.; Huang, D.; Guo, Y. Performance improvement of plug-and-play dual-phase-modulated continuous-variable quantum key distribution with quantum catalysis, *Quant. Inf. Process.* **2019**, *18*, 12372.
24. Zhong, H.; Wu, X.D.; Deng, Y.M.; Huang, D.; Xiong, S.; Guo, Y. Passive-state preparation for continuous variable quantum key distribution in atmospheric channel, *Quant. Inf. Process.* **2021**, *20*, 08258. [CrossRef]
25. Zuo, Z.; Wang, Y.J.; Liao, Q.; Guo, Y. Overcoming the uplink limit of satellite-based quantum communication with deterministic quantum teleportation. *Phys. Rev. A* **2021**, *104*, 022615. [CrossRef]
26. Mao, Y.; Wang, Y.; Huang, W.; Huang, D.; Guo, Y. Optical frequency comb-based multichannel parallel continuous-variable quantum key distribution. *Opt. Express* **2019**, *27*, 25314–25329.
27. He, Y.; Mao, Y.; Huang, D.; Liao, Q.; Guo, Y. Indoor channel modeling for continuous variable quantum key distribution in the terahertz band. *Opt. Express* **2020**, *28*, 32386–32402. [CrossRef] [PubMed]
28. Yao, K.; Wang, J.; Liu, X.; Liu, W. Closed-loop adaptive optics system with a single liquid crystal spatial light modulator. *Opt. Express* **2014**, *22*, 17216–17226. [CrossRef] [PubMed]
29. Cao, J.; Zhao, X.; Li, Z.; Liu, W.; Song, Y. Stochastic parallel gradient descent laser beam control algorithm for atmospheric compensation in free space optical communication. *Optik* **2014**, *125*, 6142–6147. [CrossRef]
30. Wang, Y.; Wu, X.; Zhang, L.; Huang, D.; Liao, Q.; Guo, Y. Security analysis of passive measurement-device-independent continuous-variable quantum key distribution with almost no public communication. *Quantum Inf. Process.* **2019**, *18*, 372.